Available online at www.sciencedirect.com
SCIENCE DIRECT®
Journal of Sound and Vibration 277 (2004) 391–403
JOURNAL OF SOUND AND VIBRATION
www.elsevier.com/locate/jsvi

Harmonic response of a structure mounted on an isolator modelled with a hysteretic operator: experiments and prediction

A. Al Majid, R. Dufour*

Laboratoire de dynamique des Machines et des Structures, INSA de Lyon, UMR CNRS 5006, Batiment Jean d'Alembert, Rue des Sciences 8, Villeurbanne 69621, France

Received 18 October 2002; accepted 2 September 2003

Abstract

In a previous article the authors presented the mathematical formulation of an original and general hysteretic operator for modelling force-deflection loops, in particular of isolators, the application being concerned by transient response. In the present article the dynamic behaviour of a dry-friction isolator is investigated using a steady-state experimental force-deflection loop to determine the parameters of the first order differential equation of the proposed hysteretic operator. Extracting the classical complex stiffness from the model and comparing it to measured value permits an initial validation. The harmonic response of a cantilever beam equipped with a dry-friction isolator is then predicted by coupling the classical second order equation of the beam in bending with the first order differential equation, giving the restoring force of the isolator. The experiment described permits validating the use of the proposed hysteretic model in the case of harmonic steady state behaviour.

1. Introduction

The effects of an isolator can be introduced in the equation of motion governing the dynamic behaviour of structures by using either stiffness models (to be introduced in the left-hand side of the equations) or restoring force models (to be introduced in the right-hand side). However, from a general point of view, the dynamic behaviour of isolators is difficult to model using a deductive approach, because they are currently designed with complicated geometry and various components such as fluid, elastomer, metal cushions, etc., see Refs. [1–4]. Moreover, their

*Corresponding author. Tel.: +33-472-43-82-02; fax: +33-472-43-89-30.
E-mail address: regis.dufour@insa-lyon.fr (R. Dufour).

0022-460X/$ - see front matter
doi:10.1016/j.jsv.2003.09.025

dynamic behaviour depends on parameters such as temperature, deflection, forcing frequency, type of excitation. This leads to non-linear and dissipative behaviours. The inductive approach consists in extracting parameters from the experimental force-deflection loops. For example, by using this approach Ko et al. [5], Wong et al. [6], and Ni et al. [7] were involved in the identification of an isolator having elasto-plastic behaviour and in the harmonic response of a frame equipped with such an isolator.

Laboratory investigations have concerned the formulation of stiffness models and more recently an original restoring force model, the parameters being identified by using experimental force-deflection loops. Stiffness models require the definition of complex stiffness (i.e., dynamic equivalent stiffness and loss factor) in the case of harmonic response [8], instantaneous and tangent stiffnesses, and modal damping in the case of transient response due to random [9] or shock [10] excitations. Consequently, stiffness models are limited, in particular when different types of excitations are superposed. The restoring force model requires an equation of envelope curves and various parameters, which until today have only been used to predict transient responses [11–12]. Therefore, in this article, the restoring force model is used to predict the steady state harmonic response of a flexible structure equipped with a dry-friction isolator.

Section 2 briefly presents the proposed hysteresis model and its application to a dry-friction isolator used for on-board electronic equipment. Then, quasi-static and harmonic models are formulated on the basis of experiments. Section 4 describes the extraction of the complex stiffness from the restoring force model formulated and from the experimental loop in order to compare them and to check the isolator model taken alone. Finally, the predicted and measured harmonic responses of a beam in bending equipped with the dry-friction isolator provide an experimental validation of the isolator model coupled with the beam model.

2. Hysteretic restoring force model

In mechanical engineering real isolators have a hysteresis behaviour which can be described by a force-deflection loop. Several hysteretic models exist in the literature, but they are limited when the model has to be formulated from the envelope curves of the loop which can be time and velocity dependant. Coulomb's model is too rustic. Dalh's model has straight envelope lines while the models of Krasnosel'skii and Duhem-Madelung are much too general, see Bliman [13]. Bouc's model [14] and Wen's model [15–16] are difficult to formulate from the envelope curves.

A general hysteresis model should integrate isolator behaviour with various shapes: softening, hardening or a combination of both. In Ref. [12] the authors presented the mathematical formulation of an original and general hysteretic operator for modelling the force-deflection loop and that of isolators in particular. The idea of the model proposed stems from Dahl's model, where the envelope curves are reduced to horizontal straight lines.

Let a relation be between two scalar variables: $p \rightarrow q$. The hysteresis appears when a value of output q cannot be determined by knowledge of only one value of input p. A solution consists in introducing a local irreversibility of the relation $p, q \rightarrow \dot{q}$, and this process is used to index the information memorised. Now suppose that p and q are linear combinations of R, the restoring

force and w, the deflection:

$$p = \frac{1}{R_0}(-\lambda R + (1-\lambda)kw), \tag{1}$$

$$q = \frac{1}{R_0}((1-\lambda)R - \lambda kw), \tag{2}$$

where R_0 is a reference force, $k > 0$ has the dimension of a stiffness, while λ comprised in the interval [0,1] is a constant defining the general behaviour: $\lambda = 0$ provides a model with a pure hardening behaviour while $\lambda = 1$ provides a model with a pure softening behaviour. Consequently the hysteretic operator is defined by the following first order equation:

$$\frac{dq}{dt} = \alpha\frac{dp}{dt}(h - q\,\mathrm{sgn}(\dot{p}))^{\mu}, \tag{3}$$

where α is a dissipation energy constant, μ, is the rotation constant of the loop, and h is the equation of the upper and lower envelope curves between which function q is obliged to remain.

The originality of the proposed model in comparison to existing models, lies mostly in the use of envelop curves, with constants α, μ and k having a well defined role. In addition the proposed model is time and velocity dependant, thereby making the model more general. Measurement of the force-deflection loops permits the identification of these parameters, in particular the envelope curves.

3. Isolator modelling

The proposed hysteretic model is applied to an all-metal isolator commonly used in the passive isolation of on-board electronic equipment; Fig. 1 shows its photograph (a) and its diagram (b). It works mainly in traction-compression and has a double end-stop. Its aluminium housing is 22.5 mm high and has a diameter of 28.5 mm. Two conical springs and two cushions made of metal wires provide the restoring force. Micro-friction between the metal wires of the cushions

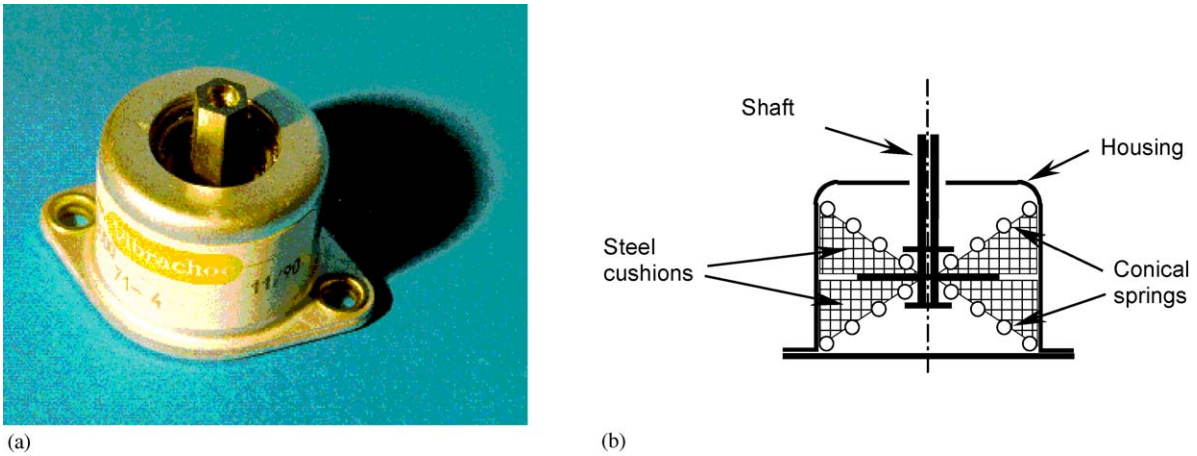

Fig. 1. Photograph (a) and diagram (b) of the all-metal isolator.

and friction between the cushions and housing cause the dissipative effect. This design permits obtaining a dissipative hardening–hardening behaviour which is described by a force-deflection loop bounded by two vertical asymptotic lines.

In what follows, experimental quasi-static and harmonic force-deflection loops are successively used to define the model parameters. Moreover, the equivalent stiffness and loss factor are extracted from the simulated and measured loops in order to enhance the validation of the model.

3.1. Quasi-static modelling

The isolator is subjected to five cycles obtained by imposing a deflection of 20 mm/min. The first-four force-deflection cycles are devoted to the warm-up while the last one, shown in Fig. 2(a), is used for modelling. The vertical asymptotic behaviours at a deflection of $+/-6$ mm are caused by the double end-stop. It should be observed that high deflection induces high stress in the cushions and consequently a high dissipative effect within the ranges of deflection closed at the end-stops, i.e. (-6 mm, -4 mm) and (4 mm, 6 mm).

The measured quasi-static loop is used to adjust the parameters of the isolator model. The hardening effect is obtained with $\lambda = 0$ which is introduced in relations (1) and (2). Consequently, Eq. (3) becomes

$$\frac{\mathrm{d}R}{\mathrm{d}t} = \alpha k \frac{\mathrm{d}w}{\mathrm{d}t}\left(h - \frac{R}{R_0}\,\mathrm{sgn}\left(\frac{k\dot{w}}{R_0}\right)\right)^{\mu}. \tag{4}$$

Several numerical tests permit evaluating the remaining constants:

$$\alpha k = 45{,}500, \quad R_0 = 1, \quad \mu = 1. \tag{5}$$

The envelope function h is given by

$$h = \frac{(h_u + h_\ell)\,\mathrm{sgn}(\dot{w}) + (h_u - h_\ell)}{2}, \tag{6}$$

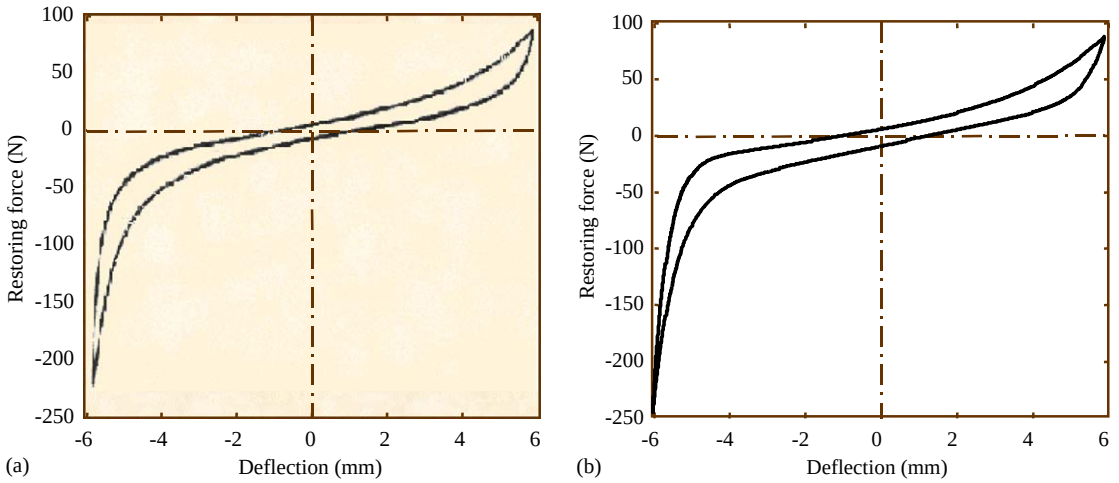

Fig. 2. Measured (a) and simulated (b) quasi-static loops.

with the lower h_l and upper h_u envelope curves approximated by the least-square method:

$$h_l = -8.63 + 7080.2w - 0.01e^{-1650\,w} + 0.00025e^{2050w}, \tag{7}$$

$$h_u = 1.12 + 4307.8w - 0.00005e^{-2550w} + 3.68e^{470w}. \tag{8}$$

Fig. 2(b) shows that the loop obtained by forcing the deflection in relation (4) is close to the measured loop shown in Fig. 2(a).

3.2. Harmonic modelling

After warming up, force-deflection loops measured at three forcing frequencies (20, 30 and 50 Hz) highlight frequency independence and deflection dependence. Fig. 3(a) presents force-deflection loops measured at a 20 Hz forcing frequency and obtained for several amplitudes of the deflection. The model keeps the same shape as previously: there is a hardening effect with the deflection. The behaviour is quasi elastoplastic.

The harmonic model of the isolator is also formulated with Eq. (3) but the parameters are evaluated as follows:

$$\alpha k = 87{,}500, \quad R_0 = 1, \quad \mu = 1. \tag{9}$$

The envelope function h has expression (6) but its lower and upper envelope curves approximated by the least squared method are given by

$$h_l = (0.003 + 0.001e^{-w} - 0.001e^{w})e^{2w_c} - (31.8 - 16.3e^{-w} - 26e^{w})e^{-2w_c} - (3.03 + 4.3e^{-w} + 1.8e^{w}), \tag{10}$$

$$h_u = (0.004 + 0.001e^{-w} - 0.001e^{w})e^{2w_c} + (25.2 - 19.1e^{-w} - 8.3e^{w})e^{-2w_c} + (5.5 - 4.4e^{-w} + 1.5e^{w}), \tag{11}$$

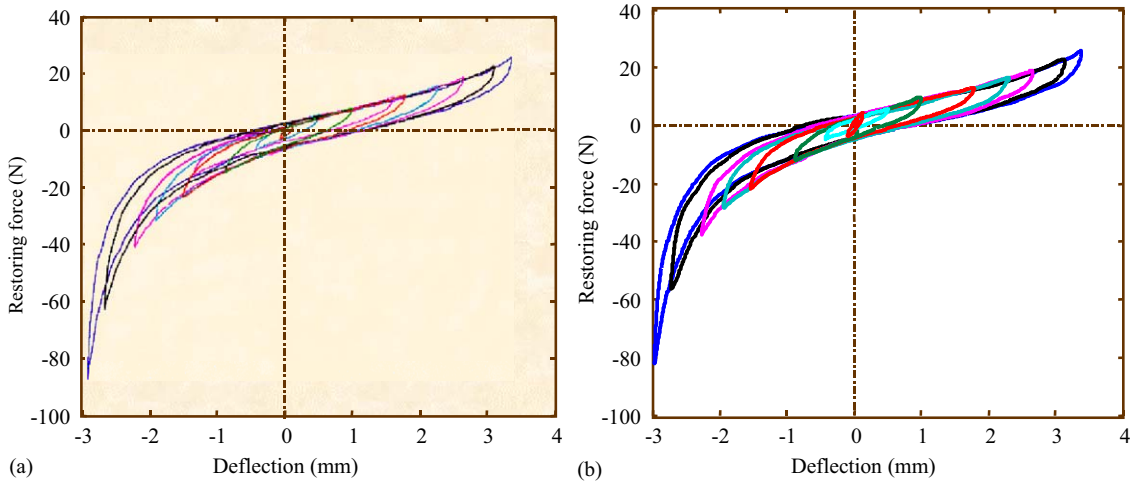

Fig. 3. Measured (a) and simulated (b) harmonic loops.

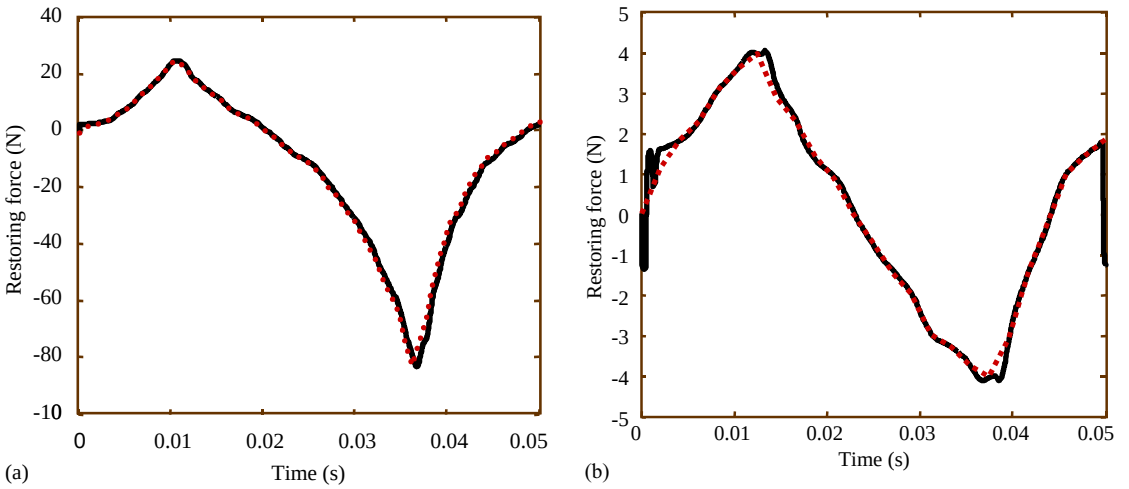

Fig. 4. Time history of the measured (dot line) and simulated (solid line) restoring forces for (a) high and (b) low deflections.

where deflection w is expressed in mm, and w_c are the maximum deflections of the experimental loops which are used to update the model's parameters. Fig. 3(b) shows the force-deflection loops simulated by forcing the deflection in the harmonic model. The comparison of the measured and simulated loops, see Fig. 3(a) and (b), show that the model is satisfactory. This is better highlighted by comparing the time history of the measured and simulated restoring forces for low deflection, Fig. 4(a), or high deflection, Fig. 4(b). The good agreement permits an initial validation, confirmed in the following sub-section by the consideration on complex stiffness.

3.3. Complex stiffness

Classically, harmonic investigation requires the use of dynamic equivalent stiffness k_e and loss factor η_e which are assumed to be constant during one cycle, see for example Ref. [1]

$$k_e = \frac{F_{max} - F_{min}}{w_{max} - w_{min}}, \tag{12}$$

$$\eta_e = \frac{(F_{max} - F_{min})|_{w=0}}{F_{max} - F_{min}}. \tag{13}$$

Relations (12) and (13) permit the formulation of the complex stiffness k:

$$k = k_e(1 + \mathrm{j}\eta_e), \tag{14}$$

with $\mathrm{j} = \sqrt{-1}$.

Applying formula (12) and (13) to the measured and simulated quasi-static loops presented in Fig. 3 gives $k_e = 26{,}135\,\mathrm{N/m}$ and $\eta_e = 0.039$ for the measured loop and $k_e = 26{,}750\,\mathrm{N/m}$ and $\eta_e = 0.038$ for the simulated loop.

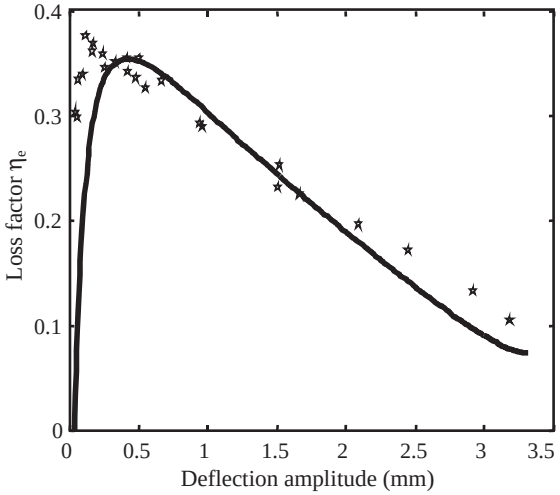

Fig. 5. Loss factor extracted from the experiment (dotted line) and from the model (solid line).

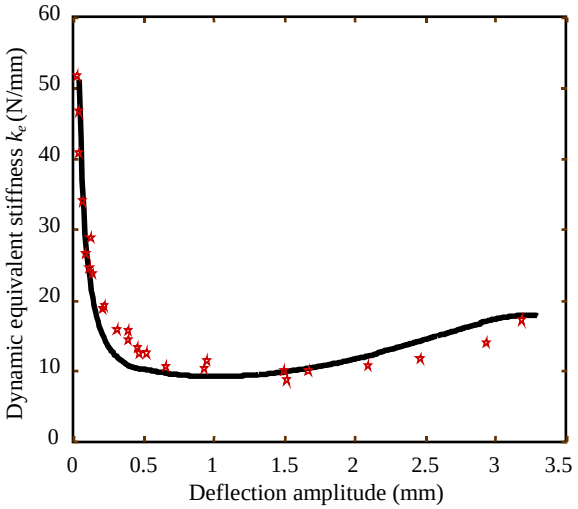

Fig. 6. Dynamic equivalent stiffness versus deflection extracted from the experiment (dotted line) and from the model (solid line).

Moreover, Figs. 5 and 6 show the dynamic equivalent stiffnesses and the loss factors respectively, extracted from the simulated and measured loops presented in Fig. 3, by using relations (12) and (13) respectively. The dynamic equivalent stiffness is maximum at low amplitudes of deflection, damping decreases with large deflections.

The satisfactory agreement concerning both quasi-static and harmonic loops permit declaring that the restoring force model proposed is reliable enough to be implemented in a flexible structure subjected to a harmonic excitation. This is done in the next section.

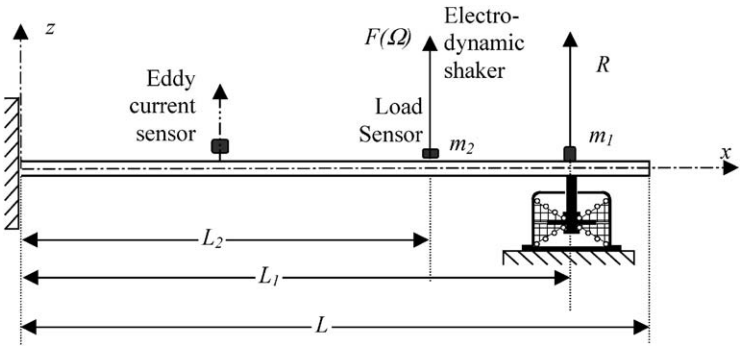

Fig. 7. Beam-isolator system in bending.

4. Harmonic response of a beam-isolator system

The harmonic response of a beam, see Fig. 7, equipped with the isolator described previously is carried out numerically and experimentally.

4.1. Experimental set-up

The beam, made of steel, (cross-section area S, area moment of inertia I, mass density $\rho = 7800\,\mathrm{kg/m^3}$, Young's modulus $E = 2 \times 10^{11}\,\mathrm{N/m^2}$, length $L = 0.375\,\mathrm{m}$, thickness 0.004 m and width 0.040 m), is clamped at one end and the dry-friction isolator is located at the abscissa $L_1 = 0.335\,\mathrm{m}$. The transverse harmonic excitation caused by a suspended electrodynamic shaker is applied on a piezoelectric load sensor stuck at the abscissa $L_2 = 0.165\,\mathrm{m}$. The lateral displacement is measured using a proximity probe facing the abscissa 0.099 m. The on-board masses of the isolator and of the load sensor are respectively $m_1 = 2 \times 10^{-3}$ and $m_2 = 22.1 \times 10^{-3}\,\mathrm{kg}$. The damping of the beam alone is evaluated by using measured modal factors. An experimental forced response frequency of the cantilever beam with no isolator and subjected to a harmonic sine wave excitation gives the first six modal viscous factors:

$$\boldsymbol{\alpha} = [\,0.0052 \quad 0.0005 \quad 0.0007 \quad 0.0004 \quad 0.0022 \quad 0.0040\,]. \tag{15}$$

4.2. Modelling

The effect of the isolator is taken into account by using its restoring force and not by using its complex stiffness. The beam is modelled using the Rayleigh–Ritz method. Functions of displacement $\phi_i(\xi)$ are kinematically admissible, where $\xi = x/L$ is the non-dimensional variable of space, and functions of time $z^i(t)$ permit the expansion of the lateral displacement $w(\xi, t)$ which has the following expression when repeated indices are used:

$$w(\xi, t) = \phi_i(\xi)\, z^i(t). \tag{16}$$

The displacement function chosen have a polynomial expression: $\phi_i(\xi) = \xi^{1+i}$ with $i > 0$. Seeking the expressions of the kinetic and strain energies and of the virtual work of the applied

forces and applying the Lagrange equations yield the system of differential equations:

$$M_{ij}\ddot{z}^j + K_{ij}z^j = F_i \tag{17}$$

The mass and stiffness coefficients M_{ij} and K_{ij} are given by the following formulas:

$$M_{ij} = \frac{\rho SL}{(i+j+3)} + m_1\xi_1^{(i+j+2)} + m_2\xi_2^{(i+j+2)}, \tag{18}$$

$$K_{ij} = \frac{EI}{L^3}\frac{(1+i+j+ij)ij}{(-1+i+j)}. \tag{19}$$

The applied force F_i

$$F_i = -R\xi_1^{1+i} + F(\Omega)\xi_2^{1+i} \tag{20}$$

contains the harmonic excitation force $F(\Omega)$

$$F(\Omega) = F_0\sin(\Omega t) \tag{21}$$

and restoring force R of the isolator which is obtained by coupling the first order differential Eq. (4), whose parameters are given by relations (9)–(11), with the second order Eq. (17).

The homogeneous system (17) permits formulating modal matrix $\boldsymbol{\varphi}$ containing the mode ϕ_{ij} of the beam alone. The change of variable

$$\mathbf{z} = \boldsymbol{\varphi}\mathbf{q} \tag{22}$$

introduced in the energies and virtual work yields the modal equations:

$$\mathbf{m}\ddot{\mathbf{q}} + \mathbf{c}\dot{\mathbf{q}} + \mathbf{k}\mathbf{q} = \mathbf{f}, \tag{23}$$

where modal matrices $\mathbf{m}$, $\mathbf{c}$ and $\mathbf{k}$ and modal vector $\mathbf{f}$ are formulated as follows:

$$\mathbf{m} = \boldsymbol{\varphi}^{\mathrm{t}}\mathbf{M}\boldsymbol{\varphi}, \quad \mathbf{k} = \boldsymbol{\varphi}^{\mathrm{t}}\mathbf{K}\boldsymbol{\varphi}, \quad \mathbf{f} = \boldsymbol{\varphi}\mathbf{j}^{\mathrm{t}}\mathbf{F}. \tag{24}$$

The coefficients of the diagonal damping modal matrix are formulated by using the measured modal damping given by relation (15):

$$c_{ii} = 2\alpha_i\sqrt{m_{ii}k_{ii}}. \tag{25}$$

In Ref. [12], it was demonstrated that the solution of the coupled Eqs. (4) and (17) exists and is unique.

4.3. Results

The predicted harmonic response of the beam-isolator system obeys the experimental swept-sine investigation. It is performed in the time domain: the step-by-step Runge-Kutta method is used. The forcing frequency is incremented after steady-state behaviour is reached and the amplitude of displacement recorded. For each forcing frequency Ω within the 0–250 Hz range, the initial conditions are:

$$\mathbf{z}(0) = 0, \quad \dot{\mathbf{z}}(0) = 0, \quad R(0) = 0. \tag{26}$$

During the experimental swept-sine investigation, the amplitude of the harmonic force is recorded. It is plotted in Fig. 8 and used as input data in the prediction. The predicted and measured harmonic responses are presented in Fig. 9. Two resonance phenomena are highlighted.

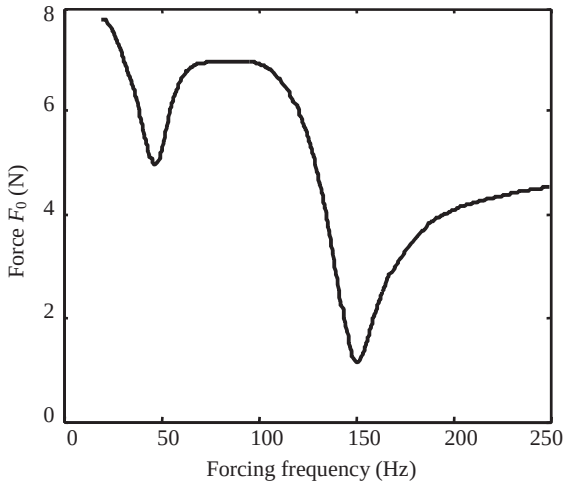

Fig. 8. Amplitude of the harmonic force versus forcing frequency.

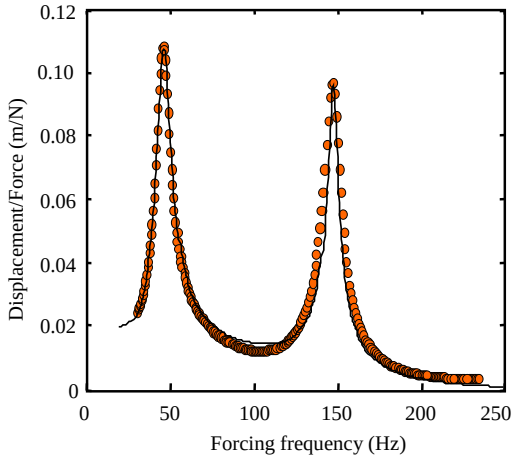

Fig. 9. Predicted (dotted line) and measured (solid line) harmonic responses of the beam-isolator system.

The fairly good agreement permits validating the model and in particular the hysteretic operator used for modelling the isolator. The force-deflection loops of the isolator generated during the simulation and plotted in Fig. 10 permit a possible dissipation evaluation.

5. Conclusions

A hysteresis operator was used to model the behaviour of an all-metal isolator. Its parameters were identified using either quasi-static or harmonic experimental force-deflection loops. The elasto-plastic behaviour of the dry-friction isolator makes it frequency independent. The complex

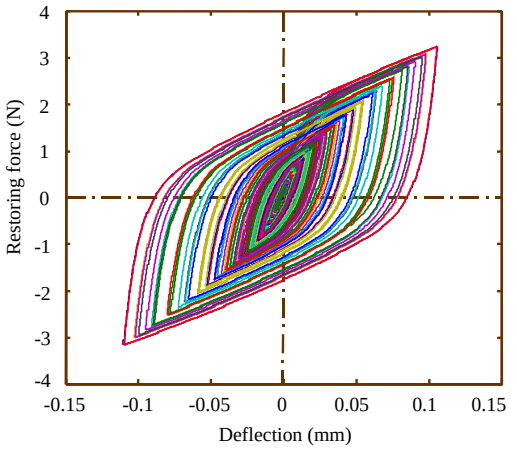

Fig. 10. Force-deflection loops of the isolator generated during the simulation.

stiffness extracted from the developed hysteretic model was compared to the experimental one. It is concluded that the two approaches yield roughly the same complex stiffness. This step constitutes a first validation of the hysteretic model.

Moreover the validation was confirmed by using an experimental investigation concerned with the harmonic response of a beam equipped with the isolator. The hysteretic model was coupled to the equation of the motion of the beam in bending.

Finally it was shown that the hysteretic operator is well adapted to the hysteretic behaviour of an isolator defined by experimental force-deflection loops. Moreover its implementation in the equation of motion of a system is done easily by using equations coupled by the restoring force.

Acknowledgements

The authors would like to thank the *Région Rhône-Alpes* Council for its support.

Appendix A. Nomenclature

α	dissipation energy constant
$\boldsymbol{\alpha}$	measured modal damping factor vector of the beam
λ	parameter defined within the [0, 1] interval
η_e	loss factor
ξ	non-dimensional variable
ρ	mass density
Ω	pulsation of the harmonic excitation force
μ	rotation constant of the loop
ϕ	displacement function
$\mathbf{c}$	modal damping matrix
E	Young's modulus

$\mathbf{f}$	force excitation vector
F_0	harmonic excitation force amplitude
F_i	applied force
F_M, F_m	maximum and minimum forces of the loop
h	envelope curves
h_l, h_u	lower and upper envelope curves
I	area moment of inertia
j	complex number
k	constant having the dimension of a stiffness
$\mathbf{k}$	modal stiffness matrix
k_e	dynamic equivalent stiffness
K_{ij}	stiffness matrix
L	length of the beam
L_1, L_2	abscissa of the locations of the dry-friction isolator and of the excitation force
$\mathbf{m}$	modal mass matrix
m_1, m_2	masses of the isolator and of the load sensor, respectively
M_{ij}	mass matrix
p, q,	input and output functions of the hysteretic operator
$\mathbf{q}$	modal co-ordinates
R	restoring force
R_0	reference force
S	cross-section area
w	deflection
w_c	maximum deflections of the experimental loops
w_M, w_m	maximum and minimum deflections of the loop
z	function of time in the Ritz method

References

[1] D. Nashif, D.I.G. Jones, J.P. Henderson, *Vibration Damping*, Wiley, New York, 1985.
[2] M. Lalanne, Modelling damping in mechanical engineering structures, *Shock and Vibration Journal* 7 (1) (2000) 29–37.
[3] D.G. Jones, *Handbook of Viscoelastic Vibration Damping*, Wiley, New York, 2001.
[4] J.B. Roberts, P.D. Spanos, *Random Vibration and Statistical Linearisation*, Wiley, New York, 1990.
[5] J.M. Ko, Y.Q. Ni, Q.L. Tian, Hysteretic behaviour and empirical modelling of a wire-cable vibration isolator, *The International Journal of Analytical and Experimental Modal Analysis* 7 (2) (1992) 111–127.
[6] W. Wong, Y.Q. Ni, J.M. Ko, Steady-state dynamic response of structures with non-linear hysteretic isolators, *Modal Analysis: The International Journal of Analytical and Experimental Modal Analysis* 8 (1) (1993) 63–78.
[7] Y.Q. Ni, J.M. Ko, C.W. Wong, Identification of non-linear hysteretic isolators from periodic vibrations tests, *Journal of Sound and Vibration* 217 (4) (1999) 737–756.
[8] K. Gjika, R. Dufour, Rigid Body and nonlinear mount identification: application to onboard equipment with hysteretic suspension, *Journal of Vibration and Control* 5 (1) (1999) 75–94.
[9] Y. Rémouga, R. Dufour, Response of a non-linear mechanical system to an accelerogram of known PSD (in French), *Mécanique Industrielle et Matériaux* 49 (2) (1996) 110–112.

[10] K. Gjika, R. Dufour, G. Ferraris, Transient response of structures on viscoelastic or elastoplastic mounts: prediction and experiment, *Journal of Sound and Vibration* 198 (3) (1996) 361–378.
[11] A. Al Majid, R. Dufour, A restoring force model to predict the shock response of a structure on dry-friction mount (in French), *Mécanique Industrielle et Mécanique* 51 (2) (1998) 80–82.
[12] A. Al Majid, R. Dufour, Formulation of a hysteresis restoring force model. Application to vibration isolation, *Nonlinear Dynamics* 27 (2002) 69–85.
[13] P.A. Bliman, Etude Mathématique d'un Modèle de Frottement Sec: Le Modèle de P.R. Dahl, Thèse de Doctorat en Mathématiques et Automatique, University of Paris IX-Dauphine, 1990.
[14] R. Bouc, Forced vibrations of a mechanical system with hysteresis, Abstract, *Proceedings of 4th Conference on Non-linear Oscillation*, Prague, Czechoslovakia, 1967, p. 315.
[15] Y.K. Wen, Method for random vibration of hysteretic system, *Journal of the Engineering Mechanics Division, American Society of Civil Engineers* 102 (2) (1976) 249–263.
[16] Y.K. Wen, Equivalent linearisation for hysteretic system under random excitation, *Journal of Applied Mechanics* 47 (1990) 150–154.